Unravelling quantum chaos using persistent homology

Harvey Cao [1,*] Daniel Leykam [1,†] and Dimitris G. Angelakis[1,2,3,‡]

[1]*Centre for Quantum Technologies, National University of Singapore, 3 Science Drive 2, 117543 Singapore*
[2]*School of Electrical and Computer Engineering, Technical University of Crete, Chania 73100, Greece*
[3]*AngelQ Quantum Computing, 531A Upper Cross Street No. 04-95 Hong Lim Complex, 051531 Singapore*

Topological data analysis is a powerful framework for extracting useful topological information from complex data sets. Recent work has shown its application for the dynamical analysis of classical dissipative systems through a topology-preserving embedding method that allows reconstructing dynamical attractors, the topologies of which can be used to identify chaotic behavior. Open quantum systems can similarly exhibit nontrivial dynamics, but the existing toolkit for classification and quantification are still limited, particularly for experimental applications. In this paper, we present a topological pipeline for characterizing quantum dynamics, which draws inspiration from the classical approach by using single quantum trajectory unravelings of the master equation to construct analog quantum attractors and extract their topology using persistent homology. We apply the method to a periodically modulated Kerr-nonlinear cavity to discriminate parameter regimes of regular and chaotic phases using limited measurements of the system.

I. INTRODUCTION

Classical nonlinear systems can exhibit chaotic behavior if they possess extreme sensitivity to initial conditions and are topologically mixing. The interplay of these two properties leads to long-term unpredictability and seemingly random dynamics, despite being fully deterministic. When dissipative effects play a role, a complex geometrical structure can be observed in the phase-space dynamics, known as a strange attractor. Strange attractors differ from other phase-space attractors in that two points that are initially nearby on the attractor will eventually evolve to become arbitrarily far apart. This divergence is used as a diagnosis of whether a particular system is chaotic, quantified in conventional methods by calculating the maximal Lyapunov exponent (LE), a measure of the average rate of divergence in phase space [1].

When quantum effects are significant, chaotic behavior at the wave-function level is precluded due to the linearity of the Schrödinger equation [2]. Instead, the role of chaos in quantum mechanics is studied by identifying signatures of quantum systems which result in a classical counterpart that yields chaotic dynamics. Early efforts in quantifying quantum chaos focused on the spectral statistics of chaotic Hamiltonians, with level-spacing statistics corresponding to that of random matrices when the classical limit is chaotic [3–5]. There have also been various quantum generalizations of the classical LE constructed in terms of quasiclassical phase-space dynamics, the stochastic Schrödinger equation, and, more recently, out-of-time-order correlators (OTOCs) [6–9]. Beyond addressing fundamental questions concerning the correspondence principle between quantum and classical limits [10], there is interest in understanding the role of quantum chaos in the thermalization of quantum many-body systems and subsequent implications for quantum information and near-term quantum computation [11–15].

In comparison to the classical case, where the maximal LE can be used unambiguously as an indicator of chaos, the tool set for quantifying chaos in open quantum systems remains limited. Furthermore, these methods typically involve quantifiers that are difficult to measure in real experimental settings. For example, calculating the recently proposed OTOC-based LEs requires the ability to precisely reverse the evolution of a system, which is extremely challenging [16,17].

Recently, there has been growing interest in topological data analysis (TDA) methods for approaching problems in physics where geometric structure and symmetries can be exploited [18–20]. TDA is a powerful and robust framework that enables the extraction of useful and explainable topological information from complex high-dimensional data sets. One such application has been in the characterization of classical dynamical systems through counting the number of low-dimensional holes of reconstructed attractors [21–24]. This offers an alternative to methods based on calculating the maximal LE, which can be heavily affected by noise and finite data sizes [25,26].

The primary objective of this paper is to see whether TDA-based methods for chaos detection which have already proven effective in the classical case can be applied to the harder-to-visualize dynamics of open quantum systems, where the attractor in phase space is no longer well-defined by trajectories as in the classical case. As single system trajectories are

*harvey.cao@u.nus.edu
†daniel.leykam@gmail.com
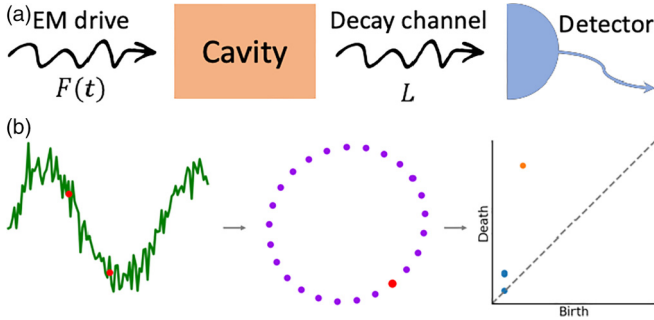‡dimitris.angelakis@gmail.com

FIG. 1. Schematic of (a) leaky periodically driven nonlinear cavity model and (b) TDA pipeline for a noisy periodic time series (left) embedded into two dimensions using time-delay embedding (middle) with the presence of a single cycle indicated by the corresponding persistence diagram (right) with 0D (blue) and 1D (orange) features. To illustrate the embedding of two points (red) in the time series according to Takens' embedding, the corresponding two-dimensional point (red) is indicated on the point cloud.

compared in the classically chaotic case to find exponential divergence, it seems sensible to adopt a quantum approach that does likewise. Thus, we propose an approach based on quantum trajectories that are obtained from unravelling methods. Specifically, we consider the Monte Carlo wave-function method, which replaces the original master equation with an ensemble of stochastically evolving quantum trajectories, whose average recovers the full density operator evolution [27,28]. We follow one member of the ensemble and use the time evolution of suitable observables to approximate a classical trajectory analog.

We apply this approach to probe the structural stability of cavitylike open quantum systems to detect transitions to quantum chaos (that is, regimes where the classical counterpart is chaotic); namely, we consider a Kerr-nonlinear cavity driven by a periodically modulated external electromagnetic field and show that the topological properties of a single quantum trajectory can be used to distinguish between regular and chaotic parameter regimes of the system. These quantum trajectories can be realized in continuous monitoring schemes, which opens a route for the application of this topological approach in real-life experimental setups [29,30]. A graphical schematic of the full pipeline is shown in Fig. 1. From a broader perspective, this paper also bridges the application of TDA to quantum dynamics and we foresee that further research surrounding this connection will be fruitful.

The outline of this paper is as follows: Section II provides a brief introduction to attractor reconstruction using time-delay embedding and the TDA method of persistent homology. Section III establishes the quantum system (and its classical counterpart) considered in the current study and introduces the Monte Carlo wave-function method. Sections IV and V present the proposed topological approach for identifying regular and chaotic regimes in classical and quantum systems, respectively, demonstrating examples of the full pipeline. Section VI summarizes the results obtained using this approach to detect chaotic phases in the parameter space of the system. Section VII makes concluding remarks and suggests future directions.

II. BACKGROUND

A. State space reconstruction

In general, the attractor of a classical dynamical system may not be directly accessible in an experimental setup because a mathematical description of the system and the dimensionality of its full phase space is unknown. Typically, measurements may only be able to be recorded of one relevant quantity at regular time intervals, resulting in a single time series $x(t)$ that represents a scalar observation function of the full state vector $\mathbf{x}(t)$:

$$x(t) = F(\mathbf{x}(t)). \qquad (1)$$

Takens' embedding theorem implies that this single time series that has been observed from a potentially unknown dynamical system can be useful in reconstructing the attractor for the full system [31]. Specifically, the observed time series $x(t)$ can be embedded into a d-dimensional vector space in such a way as to preserve the topological properties of the *full* state space $\mathbf{x}(t)$. This *time-delay embedding* involves taking uniformly time-lagged samples of the time series and concatenating them into a single vector,

$$\mathbf{X}(t) = (x(t), x(t-\tau), \ldots, x(t-(d-1)\tau)), \qquad (2)$$

where d is the embedding dimension and τ is the embedding time delay. The embedded points form features, such as loops and voids, that reflect the same topology as the attractor of the dynamical system, guaranteed by Takens' theorem as long as appropriate embedding parameters are chosen [1,31]. There is no consensus on the most favorable way to choose these and it is largely dependent on the specifics of the data, but popular heuristic methods include using mutual information for estimation of the optimal time delay and false nearest neighbors for determination of a proper embedding dimension [32,33].

B. Topological data analysis and persistent homology

TDA deals with attaching topological structure to finite sets of data, so invariant properties under smooth deformation can be derived algebraically. These structures are known as *simplicial complexes*, and can be constructed given any set of data that is equipped with some measure of distance. This triangulationlike procedure results in a network of *k-simplices*, which are sets of $k + 1$ of the points. For example, 0-simplices are points, 1-simplices are edges between pairs of points, 2-simplices are areas enclosed by three points, and so on. The condition under which k-simplices are formed from a finite set of points is chosen by the user, which consequently determines the k-simplices included in the simplicial complex. A common choice is the Vietoris-Rips (VR) complex which is built by forming k-simplices from sets of points whose pairwise distances are less than or equal to ε, a given non-negative filtration parameter (also referred to as a characteristic scale). The VR filtration is used in the present paper and illustrated in Fig. 2. The reader should note that for much larger data sets, the exponential increase in the number of simplices makes computation extremely inefficient and other, more efficient, complexes can be used such as the witness complex, which builds the complex using a subset of the original data [34].
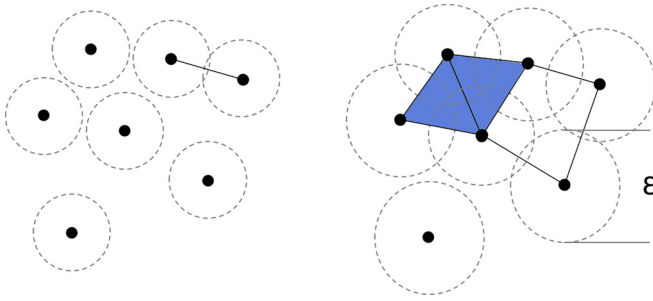
FIG. 2. Simplicial complexes constructed at a small (left) and large (right) value of the filtration parameter ϵ. Sets of k points are connected together by $k - 1$ simplices (edges, faces, etc.) if all the points in the set have pairwise intersecting ϵ balls, corresponding to the Vietoris-Rips filtration.

Over varying values of ε, a sequence of simplicial complexes can be obtained, known as a *filtration*. Each complex in the filtration will have different topological information which can be extracted to determine the abstract shape of that complex. One such nontrivial topological property is the number of k-dimensional "holes," which can be determined by calculating the kth Betti number of the complex using techniques from algebraic homology [35]. By tracking how the topology of the simplicial complex varies with the filtration parameter ε, we can effectively study what the shape of the data set looks like at different scales. This method is known as *persistent homology*, and allows a degree of importance to be attributed to topological features based on how far through the filtration they persist. The jargon refers to ranges of ε as lifetimes, with topological features being born or created at a particular value and dying or destroyed at another. Qualitatively, features that have short lifetimes we attribute to noise, while those that live longer correspond to the true topological features of the data set that we are aiming to discover.

In the above discussion, we aim to introduce the method of persistent homology, although it is by no means a comprehensive introduction. We refer the reader to the following literature which provide more in-depth and mathematical coverage, if this is needed [19,20,36].

III. MODEL

For our quantum system of interest, we consider a damped, driven, Kerr-nonlinear cavity which is known to be chaotic in the classical case and whose chaotic regimes have been well studied in the literature [37,38]. Its unitary dynamics is governed by the following Hamiltonian, written in a frame rotating with the cavity resonance frequency ω:

$$H = \tfrac{1}{2}\hbar\chi a^{\dagger 2} a^2 + i\hbar F(t)(a^\dagger - a), \qquad (3)$$

where $a^\dagger$ (a) are photon creation (annihilation) operators, respectively, χ is the photon interaction strength, $F(t)$ describes the periodic modulation by an external driving field, and time t is normalized by the cavity period $2\pi/\omega$. We consider the same driving as in Ref. [38], where $F(t)$ is a string of rectangular pulses of amplitude A, length $T/2$, and separation $T/2$, such that $F(t) = F(t + T)$. Note that if $F(t)$ is time inde-

pendent, the system loses the potential for exhibiting chaotic behavior.

Next, we incorporate damping of the cavity field into the model using the conventional formalism of open quantum systems. The time evolution of the reduced density matrix ρ describing the cavity state is governed by a master equation of the Lindblad form [27]:

$$\frac{\partial \rho}{\partial t} = -\frac{i}{\hbar}[H, \rho] + \mathcal{L}[\rho]. \qquad (4)$$

The second term on the right-hand side of Eq. (4) captures the weak coupling of the system to the environment by a set of jump operators L_i. In general, there can be many of these operators which describe different classes of system-environment couplings. Ignoring this term simply reduces Eq. (4) to the familiar von Neumann equation, capturing the unitary dynamics of the system described by the Hamiltonian (3). Here, only single photon emissions described by the jump operator L are considered and the dissipative term in Eq. (4) can be expressed as

$$\mathcal{L}[\rho] = L\rho L^\dagger - \tfrac{1}{2}\{L^\dagger L, \rho\}, \qquad (5)$$

where $\{A, B\} = AB + BA$. The effect of damping manifests as photon emissions from the leaky cavity, represented by a jump operator $L = \sqrt{\gamma}a$, where γ is a dissipative coupling constant. We assume that the pumping rate of photons into the cavity from the thermal environment is zero, following Refs. [38,39].

Though the master Eq. (4) can be solved numerically, if the relevant Hilbert space of the quantum system is of dimension N, the density operator requires N^2 real numbers to represent. This heavy computational requirement can be reduced using the quantum jump (Monte Carlo wave function) method, which constructs quantum trajectories by evolving wave functions $|\psi(t)\rangle$ using a pseudo-Hamiltonian of the form

$$H_{MC} = H - \frac{i\hbar}{2}L^\dagger L, \qquad (6)$$

combined with stochastic jumps that correspond to the environmental action of the jump operator(s). Averaged over an ensemble of many trajectories, this evolution becomes equivalent to the master equation treatment in Eq. (4) [28,40]. Expectation values of observables $\hat{O}$ are similarly calculated by using the expectation values of wave functions $\langle \psi(t)|\hat{O}|\psi(t)\rangle$ and taking the ensemble mean over all trajectories. Importantly, this method allows for mimicking the behavior of individual realizations of the system dynamics and correctly reproduces the density matrix when averaged over many iterations.

In the classical limit of large amplitude coherent states, when the average number of photons in the cavity tends to infinity, following Refs. [37–39], the master Eq. (4) can be transformed into

$$\frac{d\xi}{dt} = -\frac{1}{2}\gamma\xi + F(t) - i\chi|\xi|^2\xi, \qquad (7)$$

where ξ is a complex dynamical variable whose real and imaginary components represent the position and momentum, respectively. This variable can be compared directly with the expectation value of the photon annihilation operator $\langle \hat{a} \rangle_\psi$ in the quantum case. The nonlinear dynamical system described
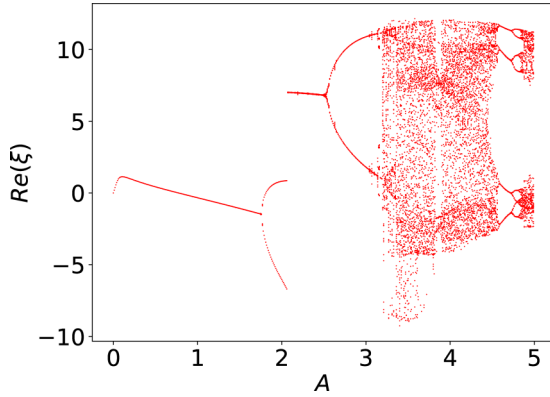
FIG. 3. Stroboscopic values of $\mathrm{Re}(\xi)$ at integer multiples n of the driving period $40 < n < 100$ as a function of the driving amplitude A. This classical bifurcation diagram visually indicates the transitions between regular and chaotic behavior. Simple curves correspond to regular periodic dynamics and the thicker bands correspond to chaotic trajectories which wander densely in the phase space. The driving period is fixed at $T = 8$ and other model parameters have values of $\gamma = 0.05$ and $\chi = 0.008$.

by Eq. (7) can be shown to exhibit regions of chaotic behavior, as visualized in the bifurcation diagram (Fig. 3) that shows the stroboscopic parameter dependence. Simple curves correspond to regular dynamics, while thicker bands indicate an exploration of the phase space that is characteristic of chaotic behavior.

IV. CLASSICAL CHAOS DETECTION

The attractor of a dissipative system describes its long-time evolution in phase space and has distinct topological properties based on whether the system dynamics exhibit regular (nonchaotic) or chaotic behavior. As discussed in Sec. II A, an attractor can be faithfully reconstructed (up to its topology) from the time series of a single observable through an embedding technique, without knowledge of the full phase-space dynamics. The resulting embedded data can then be analyzed through TDA methods such as persistent homology to characterize the reconstructed attractor and thus the system of interest. This method has been previously proposed as a quantifier for classical chaos as an alternative to the maximal LE, which can be difficult to compute for noisy, finite data [21,22].

Recall from the Introduction that in the study of quantum chaos, we are interested in finding signatures of the quantum system in regimes where the corresponding classical system is chaotic. Thus, we start with an analysis of the classical limit described by Eq. (7) and use it to determine the parameter regimes under which the system exhibits chaos.

The embedding and TDA pipeline is demonstrated for the analysis of the classical dynamical system for drive parameter values corresponding to regular and chaotic phases in Fig. 4. In this paper, for the time-delay embeddings we determine optimal hyperparameters using the heuristic methods discussed in Sec. II. It should be noted that although the specific values of the embedding delay and embedding dimension are not important as long as they satisfy the criteria of Takens' the-
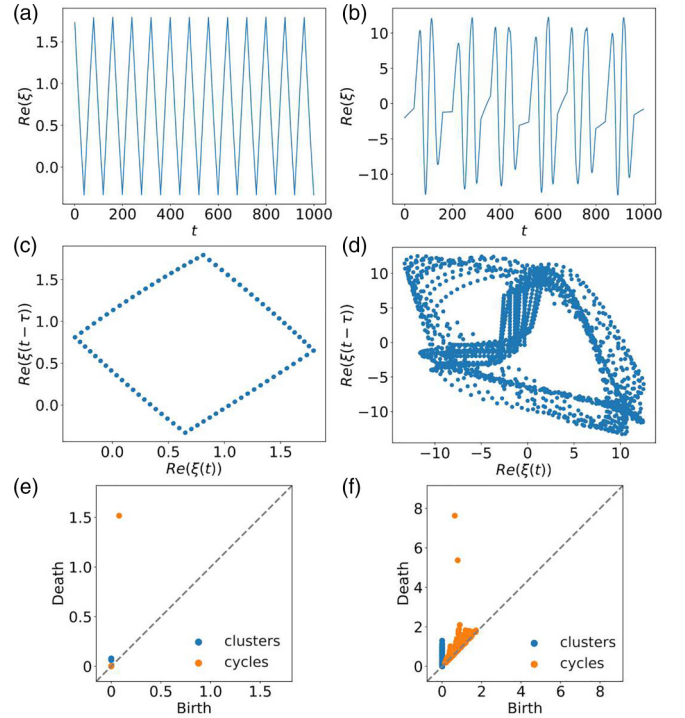

FIG. 4. Example of TDA pipeline for the classical system [Eq. (7)] in regular ($A = 1$, $T = 8$) (left) and chaotic ($A = 4.5$, $T = 8$) (right) phases. Time series evolution of real part of dynamical variable (a), (b) with corresponding two-dimensional time-delay embedding (c), (d), and persistence diagram (e), (f) for zero- (blue) and one-dimensional (orange) features. Embedding time-delay is $\tau = 20$, determined using heuristic methods (see Sec. II A).

orem [31], they do have an influence on the features obtained through persistent homology due to the discrete nature of the data. We verify in the Appendix that the results for the quantum case remain robust over a wide range of hyperparameter values.

For driving parameters chosen in the regular phase ($A = 1$, $T = 8$), the periodic dynamics obtained by numerically solving Eq. (7) and shown in Fig. 4(a) lead to a reconstructed attractor that has a simple geometric structure. The embedded point cloud shown in Fig. 4(c) exhibits a single cycle. This is quantified by the persistence diagram in Fig. 4(e) which identifies the presence of the cycle through the single long-lived one-dimensional feature furthest from the diagonal. The strange attractors that correspond to chaotic dynamics have much more complex structures whose topology cannot be described analytically as in the regular case [1]. Figure 4(b) shows the time series for parameter values chosen in the chaotic phase ($A = 4.5$, $T = 8$), which results in a reconstructed attractor whose points are scattered densely over the phase space in Fig. 4(d). Correspondingly, the persistence diagram in Fig. 4(f) indicates that at the scale of the system dynamics there are numerous features with a range of lifetimes. During the transition between the regular and chaotic phases, we note that the attractors develop two long-lived features indicative of two cycles. This is highly suggestive of period-doubling behavior on the route to chaos, also illustrated by the curve bifurcations in Fig. 3, as the correlation between

the number of cycles observed in phase space trajectories and multiperiodicity of the dynamics has been previously identified [22,41].

These distinctions between persistent features of different systems can be used as a quantifier for distinguishing regular and chaotic phases. Motivated by the significance of the size and number of cycles outlined in the above discussion, we consider as a topological measure the average lifetime of low-dimensional topological features, discussed further in Sec. VI.

V. QUANTUM CHAOS DETECTION

Turning now to the quantum case, we present an approach for detecting chaotic dynamics in open quantum systems using TDA, which draws inspiration from the classical attractor reconstruction method outlined above. The key idea is that instead of the ensemble-based master equation formulation, single quantum trajectories obtained from the quantum jump unravelling can be used as direct analogs to the trajectories in the classical formulation of chaos. Through measurement of a suitable observable, a time series can be obtained whose dynamical properties we can extract through time-delay embedding and the application of TDA as described in Sec. IV.

It has been shown previously that as an open quantum system becomes macroscopic, the behavior of observables $\langle \hat{x} \rangle$ and $\langle \hat{p} \rangle$ gradually resemble that of classical attractors in phase space [42,43]. However, at small action scales deep in the quantum regime, this classical evolution becomes blurred by decoherence and stochastic dissipative influences of the environment. Our findings suggest that the stochastic evolution of individual states is able to reflect the topology of the underlying motion, robust to the effects of quantum uncertainty. As a consequence, topological analysis of single quantum trajectories provides a quantifier for quantum chaos in open quantum systems. Without requiring the dynamics of the entire density operator, this method is computationally efficient and, more importantly, can be easily applied in experimental settings. For example, single quantum trajectories can be realized through continuous monitoring schemes such as homodyne detection or through directly measurable observables such as single photon detections (or any other decay or pump channel) corresponding to quantum jumps [29,30].

We first demonstrate this approach by considering the time evolution of the position expectation value $\langle \hat{x} \rangle$ as our observable to provide a simple comparison with the classical case in Fig. 5. The time evolution of the quantum system described by Eq. (3) is simulated using the computational library QuTiP [44]. We allow a single quantum trajectory to evolve over $T_{\text{trans}} < t < 1000\,\text{T}$, where $T_{\text{trans}} = 400\,\text{T}$ is discarded as transient behavior. We use Hamiltonian parameters $\chi = 0.008$ and $\gamma = 0.05$, which gives an average photon number of 50, and consider a truncated Hilbert space with up to $N = 300$ photons, following Ref. [39]. Using the computed wave functions which evolve stochastically under Eq. (6), we first obtain the time evolution for the position expectation value $\langle \hat{x} \rangle$ and apply time-delay embedding as before to obtain a higher-dimensional point cloud that captures an underlying topology of the system dynamics through Takens' theorem.
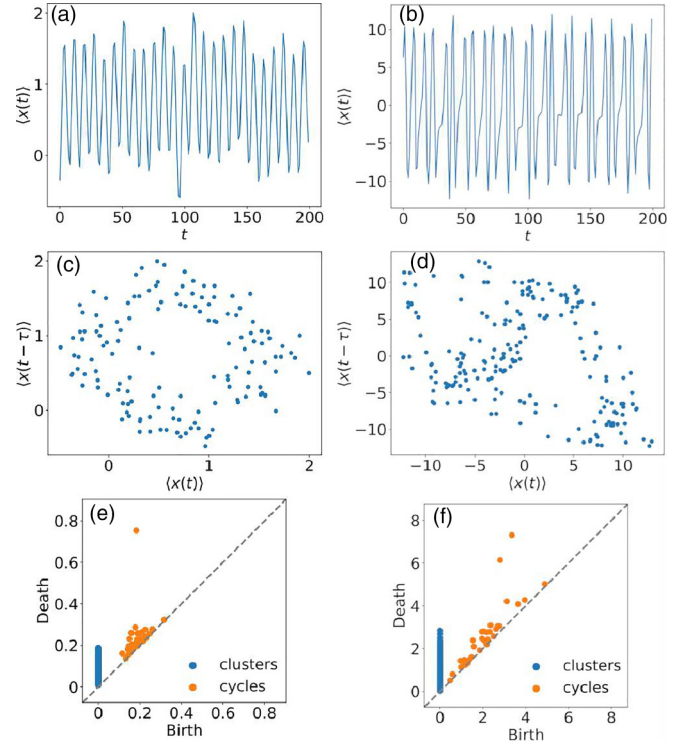

FIG. 5. Example of TDA pipeline for the quantum system [Eq. (3)] in regular ($A = 1$, $T = 8$) (left) and chaotic ($A = 4.5$, $T = 8$) (right) phases. Time series evolution of position expectation value $\langle x \rangle$ (a), (b) with corresponding two-dimensional time-delay embedding (c), (d) and persistence diagram (e), (f) for zero- (blue) and one-dimensional (orange) features. Embedding time delays are $\tau = 6$ and $\tau = 2$, respectively, determined using heuristic methods (see Sec. II A). Note that there are fewer points in the embedded cloud compared to the corresponding classical clouds due to the shorter evolution time simulated.

Since the point clouds in Figs. 5(c) and 5(d) are observed qualitatively to resemble the attractors of the dissipative classical case, we refer to them as quantum attractors. In the classical limit of large mean photon numbers, the single photon decays will enter into Eq. (7) as a shot noise term that will become negligible in the limit of an infinite number of photons, thus leading to an exact reproduction of the results in Fig. 4. For the moderate photon numbers considered here, there is an obvious smearing out of the point clouds due to quantum noise arising from fluctuations in the photon number from stochastic decay events.

Despite the presence of this noise in the quantum regime, the key result to note here is that the topological features of these noisy quantum attractors remain robust. As a consequence, these features can be extracted using persistent homology and used to differentiate dynamical phases as in the classical case discussed in Sec. IV. Here, we focus on low-dimensional features which are more efficient to compute than high-dimensional features and capture more intuitively meaningful properties of the topology. We expect, however, that higher dimensional topological features may provide additional useful insights and leave this study to future work.
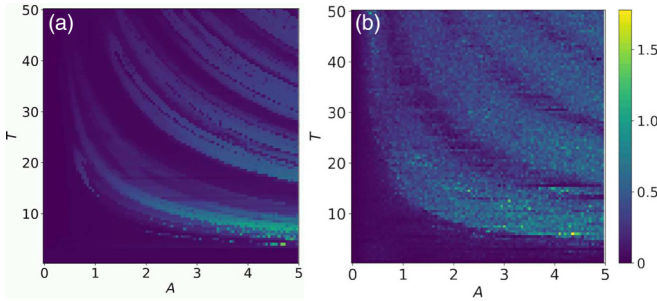
FIG. 6. Average one-hole lifetime as a function of driving amplitude A and driving period T for time evolution of (a) real part of dynamical variable for the classical system [Eq. (7)] and (b) position expectation value $\langle x \rangle$ of single Monte Carlo trajectory of quantum system [Eq. (3)].
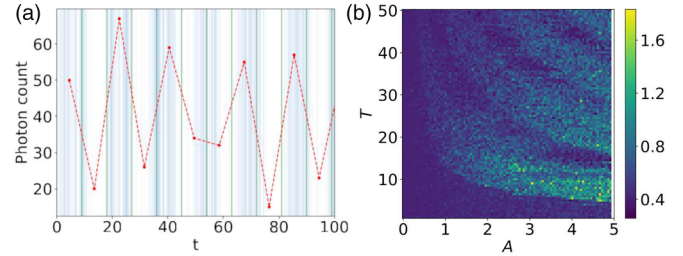

FIG. 7. (a) Binned photon count time series (red dashed line) for chaotic phase ($A = 4.5$, $T = 8$) with bin edges (green) and jump event timings (blue). (b) Average one-hole lifetime as a function of driving amplitude A and driving period T. The binning interval is fixed at 9 and embedding parameters chosen using heuristic methods (see Sec. II A).

Given that a true topological description of the dynamics has been captured, we expect the topology extracted by Takens' theorem to be independent of the observable chosen. Thus, we also consider an observable based on the count of quantum jump events, which is easier to obtain experimentally and does not interfere with the intracavity dynamics. A time series of binned photon counts is constructed by moving a sliding window across the quantum jump times, as shown in Fig. 7(a), which we then process using time-delay embedding in a similar manner. The topological summary results for both observables will be further discussed in Sec. VI.

VI. TOPOLOGICAL SUMMARIES

Various summaries can be used for quantifying the topological information of persistence diagrams, chosen depending on the specific use case [22,45,46]. Here, we consider the average lifetime of low-dimensional features in the persistence diagram, defined as

$$L_{\text{avg}}(D) = \frac{1}{|D|} \sum_{h \in D} (d - b), \qquad (8)$$

where D is the set of all features in the persistence diagram, and b (d) corresponds to the ϵ value of birth (death) of a particular feature h. This provides a summary similar to that of the Betti number and tells us the average size of topological feature in the reconstructed attractor.

It is known that under different drive parameters A and T, the quantum system of Eq. (3) contains regions of regular and chaotic behavior [39,47]. Here, we consider the driving amplitude between the range of $0 < A < 5$ and driving period between $0 < T < 50$. The average lifetime for one-dimensional holes of the reconstructed attractors are computed over this (A, T)-parameter space for both the classical and quantum systems, shown in Figs. 6(a) and 6(b), respectively. The key observation is that the distinct chaotic bands defined by different topological properties of the corresponding quantum attractors are well correlated with the dynamical phases captured by the TDA-based approach applied to the classical system. This suggests that the quantum attractors reconstructed from single quantum trajectories contain topological information about the open quantum system that can

be used to distinguish between regular and chaotic dynamics. Note that the blurring of fine structure variations of the classical dynamics within the chaotic phase bands of Fig. 6(a) are due to effects arising from the quantum-classical transition [39,48]. Additionally, we show that this measure is a robust indicator of chaos by demonstrating that the phase distinguishability is independent of free hyperparameters for the time-delay embedding as long as they satisfy the conditions for Takens' theorem (see Appendix).

Figure 7(b) shows the corresponding phase diagram obtained by considering the photon count as the observable and is similarly reminiscent of the classical phase diagram in Fig. 6(a). It should be noted that the additional free parameter of the binning interval size has a large influence on these values and the distinction between phases is somewhat less clear. The intervals need to be sufficiently large to filter out zero photon count bins, and consequently the time step size is larger than for the position operator observable, which results in fewer embedded points for a fixed evolution time. Nonetheless, we emphasize the observation that this simple measurable offers insight into a topological signature of quantum chaos and we leave it to future studies to investigate the optimal observables for probing such topologies of quantum dynamics.

VII. CONCLUSION

In this paper, we introduced a topological approach for the dynamical analysis of open quantum systems, which applies a phase-space embedding method on single quantum trajectories to construct quantum attractors and extract their topological properties using persistent homology. This was inspired by recent applications of TDA to the dynamical analysis of classical systems, underpinned by Takens' theorem, which guarantees the preservation of topology under certain transformations of time series data.

We used our quantum pipeline to investigate the dynamical phases of a leaky Kerr-nonlinear photonic cavity driven by an external field, which can exhibit chaotic behavior under certain driving parameters. Our results indicate that the single quantum trajectory retains topological information about the entire system dynamics which can be extracted to capture the regular and chaotic phases of the open quantum system.

Importantly, these topological measures are found not to be dependent on the observable considered and can be calculated using limited measurement of the system through weak continuous monitoring schemes or other directly measurable observables. Thus, the approach may present an advantage over other methods for quantifying chaos in open quantum systems, which can be experimentally difficult to realize or require measurements of the full wave function of the set of eigenstates [16,17,49–51]. Difficulties arise in part from the global nature of topological properties compared to standard LE-based techniques, which require many localized measurements to construct a suitable phase-space picture.

This paper applies the framework of TDA for the analysis of chaotic quantum dynamics. We hope that this can open another perspective for employing such topological machine-learning techniques for studying the dynamics of quantum systems, making use of their inherent robustness to noise and limited measurements, and ability to effectively handle high-dimensional data sets. Another potential application of the approach is as a data reduction step; rather than computing summary statistics of the persistence diagrams, one could feed all the obtained feature lifetimes into a machine-learning model such as an artificial neural network that could be trained to distinguish between regular and chaotic dynamics [20,51].

In this paper, we considered a system whose classical-quantum correspondence is well established, but we envision that the ideas developed in this paper can be used to study the behavior of topological properties for quantum chaotic systems without a classical counterpart such as the driven Rabi model [52] or systems in which measurement-induced back-action can modify the boundary between regular and chaotic regimes [53]. Another interesting class of systems where topological tools may be useful are those of energy-level statistics with the Brody distribution, where phase space is segmented into separate regions of regular and chaotic dynamics [54]. Since energy levels also constitute one-dimensional data, it may be possible to apply similar time-series analysis methods to distinguish between energy intervals with regular and chaotic statistics. This could be cast as a classification, clustering, or anomaly detection problem; for each of these tasks, there are well-established applications of TDA to classical data sets.

Since the TDA-based approach can be applied to both the classical and quantum regimes, another possible future route of investigation would be to see whether these topological descriptions of quantum systems can offer any insight into critical points during the quantum-classical transition. For instance, the TDA method of zig-zag persistence may provide a convenient way of tracking the persistence of specific features through a filtration of quantum attractors that correspond to changing size or action scales of the dynamical system [55,56].

Another direction for which this TDA approach may aid in uncovering unique physics is understanding quantum phase transitions in relation to the time dependence of entanglement structures, following recent work using persistent homology to extract experimentally intractable entanglement measures of quantum many-body systems [15,50,57].

Finally, we note the considerable attention given to quantum TDA algorithms as a promising candidate for near-term quantum advantage [58,59]. In particular relation to our work, a recent paper [60] establishes a quantum Takens' embedding algorithm that may expedite a search for a fully quantum pipeline for the study of quantum chaos.

APPENDIX: TIME-DELAY EMBEDDING PARAMETER DEPENDENCE

It should be noted that although the specific values of the time delay and dimension for time-delay embedding are not important as long as they satisfy the criteria of Takens' theorem [31], they do have an influence on the features obtained through persistent homology due to the discrete nature of the data.

Here, we demonstrate that the results for the quantum case remain robust over a range of hyperparameter values. Figure 8(a) shows that for a fixed embedding dimension and varying the time-delay parameter, the topological measure averaged over ten different chosen points in the regular and chaotic phases, respectively, can still be easily distinguished. Figure 8(b) indicates the same result, but with a fixed time-delay and varying the embedding dimension.
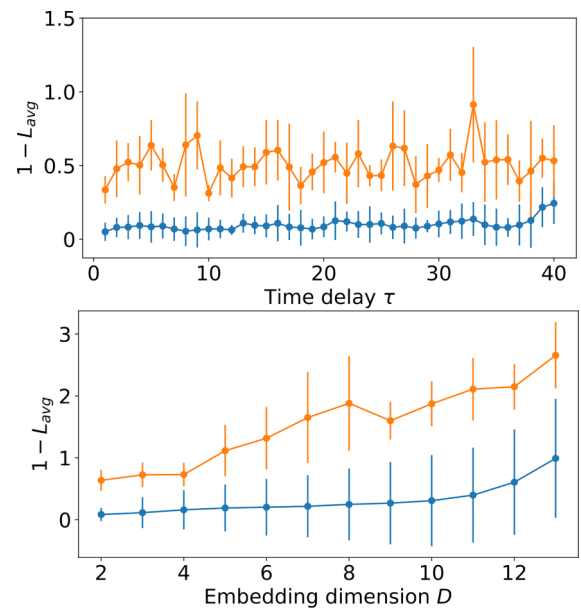

FIG. 8. Average one-hole lifetime as a function of (a) embedding time delay ($D = 2$) and (b) embedding dimension ($\tau = 7$) for position expectation value $\langle x \rangle$ of single Monte Carlo trajectory of quantum system [Eq. (3)], averaged over ten points in the regular (blue) and chaotic (orange) phases, respectively, with corresponding standard deviations.

[1] E. Ott, *Chaos in Dynamical Systems*, 2nd ed. (Cambridge University Press, Cambridge, UK, 2002).

[2] M. Berry, Quantum chaology, not quantum chaos, Phys. Scr. **40**, 335 (1989).

[3] M. V. Berry and M. Tabor, Level clustering in the regular spectrum, Proc. R. Soc. London A **356**, 375 (1977).

[4] F. Haake, M. Kuś, and R. Scharf, Classical and quantum chaos for a kicked top, Z. Phys. B **65**, 381 (1987).

[5] A. R. Kolovsky and A. Buchleitner, Quantum chaos in the Bose-Hubbard model, Europhys. Lett. **68**, 632 (2004).

[6] F. Haake, H. Wiedemann, and K. Życzkowski, Lyapunov exponents from quantum dynamics, Ann. Phys. **504**, 531 (1992).

[7] V. I. Man'ko and R. Vilela Mendes, Lyapunov exponent in quantum mechanics. A phase-space approach, Physica D **145**, 330 (2000).

[8] T. Bhattacharya, S. Habib, and K. Jacobs, Continuous Quantum Measurement and the Emergence of Classical Chaos, Phys. Rev. Lett. **85**, 4852 (2000).

[9] E. B. Rozenbaum, S. Ganeshan, and V. Galitski, Lyapunov Exponent and Out-of-Time-Ordered Correlator's Growth Rate in a Chaotic System, Phys. Rev. Lett. **118**, 086801 (2017).

[10] J. Wang, G. Benenti, G. Casati, and W.-G. Wang, Quantum chaos and the correspondence principle, Phys. Rev. E **103**, L030201 (2021).

[11] A. Sahu, S. PG, and V. Madhok, Effect of chaos on information gain in quantum tomography, Phys. Rev. E **106**, 024209 (2022).

[12] F. Borgonovi, F. Izrailev, L. Santos, and V. Zelevinsky, Quantum chaos and thermalization in isolated systems of interacting particles, Phys. Rep. **626**, 1 (2016).

[13] L. K. Joshi, A. Elben, A. Vikram, B. Vermersch, V. Galitski, and P. Zoller, Probing Many-Body Quantum Chaos with Quantum Simulators, Phys. Rev. X **12**, 011018 (2022).

[14] K. Frahm, R. Fleckinger, and D. Shepelyansky, Quantum chaos and random matrix theory for fidelity decay in quantum computations with static imperfections, Eur. Phys. J. D **29**, 139 (2004).

[15] S. Boixo, S. Isakov, and V. Smelyanskiy, Characterizing quantum supremacy in near-term devices, Nat. Phys. **14**, 595 (2018).

[16] B. Swingle, G. Bentsen, M. Schleier-Smith, and P. Hayden, Measuring the scrambling of quantum information, Phys. Rev. A **94**, 040302(R) (2016).

[17] J. Li, R. Fan, H. Wang, B. Ye, B. Zeng, H. Zhai, X. Peng, and J. Du, Measuring Out-of-Time-Order Correlators on a Nuclear Magnetic Resonance Quantum Simulator, Phys. Rev. X **7**, 031011 (2017).

[18] G. Carlsson, Topological methods for data modelling, Nat. Rev. Phys. **2**, 697 (2020).

[19] J. Murugan and D. Robertson, An introduction to topological data analysis for physicists: From LGM to FRBs arXiv:1904.11044.

[20] D. Leykam and D. G. Angelakis, Topological data analysis and machine learning, arXiv:2206.15075.

[21] S. Maletić, Y. Zhao, and M. Rajkovic, Persistent topological features of dynamical systems, Chaos **26**, 053105 (2016).

[22] K. Mittal and S. Gupta, Topological characterization and early detection of bifurcations and chaos in complex systems using persistent homology, Chaos **27**, 051102 (2017).

[23] Q. H. Tran and Y. Hasegawa, Topological time-series analysis with delay-variant embedding, Phys. Rev. E **99**, 032209 (2019).

[24] J. R. Tempelman and F. A. Khasawneh, A look into chaos detection through topological data analysis, Physica D **406**, 132446 (2020).

[25] A. Wolf, J. Swift, H. Swinney, and J. Vastano, Determining Lyapunov exponents from a time series, Physica D **16**, 285 (1985).

[26] A. Margaris, N. Kofidis, and M. Roumeliotis, A detailed study of the Wolf's algorithm, Int. J. Comput. Math. **86**, 1135 (2009).

[27] H. P. Breuer and F. Petruccione, *The Theory of Open Quantum Systems* (Oxford University Press, Oxford, UK, 2002).

[28] K. Mølmer, Y. Castin, and J. Dalibard, Monte Carlo wave-function method in quantum optics, J. Opt. Soc. Am. B **10**, 524 (1993).

[29] K. W. Murch, S. J. Weber, C. Macklin, and I. Siddiqi, Observing single quantum trajectories of a superconducting quantum bit, Nature (London) **502**, 211 (2013).

[30] S. J. Weber, K. W. Murch, M. E. Kimchi-Schwartz, N. Roch, and I. Siddiqi, Quantum trajectories of superconducting qubits, C. R. Phys. **17**, 766 (2016).

[31] F. Takens, Detecting strange attractors in turbulence, in *Dynamical Systems and Turbulence, Warwick 1980* (Springer, Berlin, 1981), pp. 366–381.

[32] A. M. Fraser and H. L. Swinney, Independent coordinates for strange attractors from mutual information, Phys. Rev. A **33**, 1134 (1986).

[33] M. B. Kennel, R. Brown, and H. D. I. Abarbanel, Determining embedding dimension for phase-space reconstruction using a geometrical construction, Phys. Rev. A **45**, 3403 (1992).

[34] V. d. Silva and G. Carlsson, Topological estimation using witness complexes, in *SPBG'04 Symposium on Point–Based Graphics 2004* (The Eurographics Association, Goslar, Germany, 2004).

[35] J. C. Friedman, Computing Betti numbers via combinatorial Laplacians, Algorithmica **21**, 331 (1998).

[36] A. Zomorodian and G. Carlsson, Computing persistent homology, Discrete Comput. Geom. **33**, 249 (2005).

[37] P. Szlachetka, K. Grygiel, and J. Bajer, Chaos and order in a kicked anharmonic oscillator: Classical and quantum analysis, Phys. Rev. E **48**, 101 (1993).

[38] T. Spiller and J. Ralph, The emergence of chaos in an open quantum system, Phys. Lett. A **194**, 235 (1994).

[39] I. I. Yusipov, O. S. Vershinina, S. V. Denisov, and M. V. Ivanchenko, Photon waiting-time distributions: A keyhole into dissipative quantum chaos, Chaos **30**, 023107 (2020).

[40] M. B. Plenio and P. L. Knight, The quantum-jump approach to dissipative dynamics in quantum optics, Rev. Mod. Phys. **70**, 101 (1998).

[41] P. S. Linsay, Period Doubling and Chaotic Behavior in a Driven Anharmonic Oscillator, Phys. Rev. Lett. **47**, 1349 (1981).

[42] T. A. Brun, I. C. Percival, and R. Schack, Quantum chaos in open systems: A quantum state diffusion analysis, J. Phys. A: Math. Gen. **29**, 2077 (1996).

[43] Y. Ota and I. Ohba, Crossover from classical to quantum behavior of the Duffing oscillator through a pseudo-Lyapunov-exponent, Phys. Rev. E **71**, 015201(R) (2005).

[44] J. R. Johansson, P. D. Nation, and F. Nori, QuTiP: An open-source Python framework for the dynamics of open quantum systems, Comput. Phys. Commun. **183**, 1760 (2012).

[45] D. Leykam and D. G. Angelakis, Photonic band structure design using persistent homology, APL Photon. **6**, 030802 (2021).

[46] I. Güzel and A. Kaygun, Classification of stochastic processes with topological data analysis, arXiv:2206.03973.

[47] I. I. Yusipov, O. S. Vershinina, S. Denisov, S. P. Kuznetsov, and M. V. Ivanchenko, Quantum Lyapunov exponents beyond continuous measurements, Chaos **29**, 063130 (2019).

[48] B. Pokharel, M. Misplon, and W. Lynn, Chaos and dynamical complexity in the quantum to classical transition, Sci. Rep. **8**, 2108 (2018).

[49] T. Macrì, A. Smerzi, and L. Pezzè, Loschmidt echo for quantum metrology, Phys. Rev. A **94**, 010102(R) (2016).

[50] P. Zanardi and N. Anand, Information scrambling and chaos in open quantum systems, Phys. Rev. A **103**, 062214 (2021).

[51] D. Huber, O. V. Marchukov, H.-W. Hammer, and A. G. Volosniev, Morphology of three-body quantum states from machine learning, New J. Phys. **23**, 065009 (2021).

[52] J. Larson, Integrability versus quantum thermalization, J. Phys. B: At. Mol. Opt. Phys. **46**, 224016 (2013).

[53] J. K. Eastman, S. S. Szigeti, J. J. Hope, and A. R. R. Carvalho, Controlling chaos in the quantum regime using adaptive measurements, Phys. Rev. A **99**, 012111 (2019).

[54] B. Batistić and M. Robnik, Dynamical localization of chaotic eigenstates in the mixed-type systems: Spectral statistics in a billiard system after separation of regular and chaotic eigenstates, J. Phys. A: Math. Theor. **46**, 315102 (2013).

[55] G. Carlsson and V. de Silva, Zigzag persistence, Found. Comput. Math. **10**, 367 (2010).

[56] S. Tymochko, E. Munch, and F. A. Khasawneh, Using zigzag persistent homology to detect Hopf bifurcations in dynamical systems, Algorithms **13**, 278 (2020).

[57] A. Piga, M. Lewenstein, and J. Q. Quach, Quantum chaos and entanglement in ergodic and nonergodic systems, Phys. Rev. E **99**, 032213 (2019).

[58] C. Gyurik, C. Cade, and V. Dunjko, Towards quantum advantage via topological data analysis, Quantum **6**, 855 (2022).

[59] I. Y. Akhalwaya, S. Ubaru, K. L. Clarkson, M. S. Squillante, V. Jejjala, Y.-H. He, K. Naidoo, V. Kalantzis, and L. Horesh, Towards quantum advantage on noisy quantum computers, arXiv:2209.09371.

[60] B. Ameneyro, G. Siopsis, and V. Maroulas, Quantum persistent homology for time series, arXiv:2211.04465.